*Chapter 1*

# RESOLVING A WORLDVIEW

Any and every 'decision-maker' gravity-bound to the planetary surface (or very nearly so) must contend with the frictional complexities confined to its relatively small surface layer. Geostrophic forces in the macroclimatic systems well-aloft set into motion processes in the planetary boundary layer that are characteristically complex and reside over many length and time scales. From the perspective of the surface-bound small autonomous flyer, however, it is the microclimatic local set of atmospheric conditions (i.e the weather) that determines the baseline flowfields within which these flyers must navigate and negotiate.

At least qualitative consideration of local weather conditions under the banner of flight safety informs human-in-the-loop-piloted (manned and remote-controlled) aircraft. For instance, human-on-board aircraft are routinely rerouted mid-flight as weather patterns evolve and if conditions are particularly austere from the onset, flights may be grounded altogether. Once nominal weather conditions are restored, these massive vehicles take to the inviscid free atmosphere to further avoid any surface friction effects. But what, then, of the small autonomous flyer[1]not fortuned enough to soar above the friction or wait for clearer skies? That is to ask what becomes of the (nearly) massless flyer confined to the atmospheric boundary layer that can neither avoid the weather nor wait for it to pass? Must it either do nothing or doom itself to failure?

The principle question of how might the weather affect a vehicles' capacity to function garners much attention early in the design cycle and again as issues (sometimes tragically) arise, but relatively little attention has been placed on the experimental strategies of how these flyers might *learn* to function in challenging scenarios *well-before* encountering them in the real-world. It therefore seems prudent to understand the fundamental fluid processes active in the high Reynolds number turbulent atmospheric boundary layer to elucidate the types of scenarios worth simulating.

[1]be it manmade (e.g. drone) or natural (e.g. birds/insects/seeds).

## 1.1 Introduction - the atmospheric boundary layer

The turbulent exchange between a planetary surface and its atmosphere defines the atmospheric boundary layer (ABL), a transitionary domain whereby the inviscid conditions of the free atmosphere gradate in some fashion to satisfy the boundary conditions at the surface. Indeed, all the kinetic energy of flowing air (i.e. wind) is transformed to thermal energy (i.e. heat) when its motion is terminated at the surface. Aside from the very thinnest layer immediately adjacent to the surface where molecular physics dominate, eddy diffusion (i.e. mixing due to eddy motions) in the ABL occurs due to a combination of frictional and convective exchanges of energy, mass, and momentum.

For a given domain of interest, the topography, distribution of roughness elements (e.g. height, fetch), and local weather conditions prevalent in that area for a given time of day (i.e. microclimates) all contribute to the complex nature of the gradation from free atmosphere to the surface. When averaged over some appreciable unit of length, say a large-area horizontal distance, and time (e.g. a day), transitions between sublayers appear gradual; fluid events near the surface, however, are characteristically intermittent (i.e. neither continuous nor steady) and agitated (i.e. exchanging/mixing). Due to the presence of both thermal kinetic energy processes (from surface heating) and mechanical kinetic energy processes (from frictional elements), the wind motions relegated to the ABL are nearly always turbulent and characterized by irregular motions containing all possible frequencies. When air motions are oriented in different directions and/or at different speeds, internal forces due to shearing can initiate dynamic instabilities that ultimately convert the mechanical kinetic energy of that collection of particles to thermal kinetic energy through the cascading nature of turbulence. These processes do occur aloft between layers of air, but are far more commonplace where air is locally slowed by a roughness element. As we continue to zoom into the various characteristic features that may come to define zones of influence within our view of the physical processes found in the innermost sublayers of a planetary atmosphere, a gradient-like partitioning is employed to better represent the length scales that emerge from the geometric dimensions of the elements within, the thicknesses of the boundary layers upon them, and the wakes of various sizes produced behind them.

## 1.2 The physical processes themselves - micrometeorology

In general, the effect of the Coriolis force cannot be ignored in the study of the physical processes of a planetary atmosphere, but its effect is not felt in the flux gradient relationship of the surface layer. From the fundamental principles of conservation of mass, momentum, and energy, equations used to model the forces and budget the energy in the ABL are made possible. At scales of interest, though some six orders of magnitude smaller than the largest-scale atmospheric processes, a macroscopic description of the fluid can still be justified[2]. Though a Lagrangian view is better aligned with the notion of a fluid consisting of a swarm of molecules, following the many parcels of fluid that make up a volume of interest is impractical, so for practical applications, descriptions of the fluid motion employ an Eulerian viewpoint, as is ultimately done herein.

**Fundamentals**

The continuity equation can be stated generally in convective form as:

$$\frac{D\rho}{Dt} + \rho\nabla \cdot \underline{u} = 0 \tag{1.1}$$

where the fluid is assumed a continuum. When taken to be incompressible but heterogeneous, that is, the density of the fluid as a whole may change one point to another but the density of a given element does not as it moves, the continuity equation reduces to:

$$\frac{D\rho}{Dt} = 0; \qquad \nabla \cdot \underline{u} = 0 \tag{1.2}$$

Then for an ideal Newtonian fluid[3], the momentum equation at any instant can be written as:

$$\rho\frac{D\underline{u}}{Dt} = -\nabla p + \rho\underline{B} + \mu\nabla^2\underline{u} \tag{1.3}$$

where the Coriolis force is neglected and in the most general sense, every macroscopic variable can be a function of location $(x, y, z)$ and time $t$, where $\rho$, $\underline{u}$, $p$, $\mu$, and $\underline{B}$ represent density, velocity, pressure, shear viscosity, and specific body force, respectively. Pressure, temperature, and density are related to one another through an equation of state. For an ideal gas,

$$p = \rho RT \tag{1.4}$$

can be used satisfactorily, $R$ being the gas constant. This is a reasonable approximation for both Earth and Mars atmospheres. For a stationary atmosphere, the vertical

[2]the Knudsen number — a comparison of the characteristic physical length scale of the fluid to that of the molecular mean free path — is typically used to determine when the treatment of the fluid as a continuous distribution of mass in space is valid. It is worth mentioning that the treatment of a fluid as a set of continuous fields (macroscopic viewpoint), though useful, does not illuminate the true particulate nature of the fluid (microscopic viewpoint) itself.

momentum component of eq. (1.3) yields $dp/dz = -\rho g$, which, through use of eq. (1.4), can be used to test the stability of an atmospheric parcel by studying the isentropic motion of a fluid particle on account of the temperature gradient as:

$$(\frac{dT}{dz})_{ad} = -\frac{g}{c_p} \tag{1.5}$$

which is known as the adiabatic lapse rate and describes a *neutrally stable* atmosphere when $dT/dz = (dT/dz)_{ad}$. If the vertical temperature gradient is greater than the adiabatic lapse rate, $dT/dz > (dT/dz)_{ad}$, then the fluid particle put into rising motion maintains a density greater than its surroundings and the atmosphere is described as *unstable*. If the fluid particle sinks, $dT/dz < (dT/dz)_{ad}$, then the reverse holds and the atmosphere is described as *stable*. Due to the significant heating from surface radiation near the surface, which changes dramatically night-to-day, air motions can be initiated even when the atmosphere is at rest (i.e. $\underline{u} = 0$).

**Scaling considerations**

Upon expanding into its differential form, and adopting these scalings:

Table 1.1: Selected scaling parameters

| Scaling parameter | Description | Scaling Substitution |
|---|---|---|
| $L$ | Characteristic length | $\underline{x} = L\underline{x}^*$ |
| $U$ | Characteristic velocity | $\underline{u} = U\underline{u}^*$ |
| $f$ | Characteristic frequency | $t = t^*/f$ |
| $\Delta p_0$ | Reference pressure difference | $p = \Delta p_0 p^*$ |
| $g$ | Gravitational acceleration | $\underline{B} = g\underline{g}^*$ |

the momentum equation (1.3) can be transformed, after rearrangement, into nondimensional form as:

$$\frac{fL}{U}\frac{\partial \underline{u}^*}{\partial t^*} + (\underline{u}^* \cdot \nabla^*)\,\underline{u}^* \;=\; -\frac{\Delta p_0}{\rho U^2}\nabla^* p^* + \frac{gL}{U^2}\underline{g}^* + \frac{\mu}{\rho U L}\nabla^{*2}\underline{u}^* \tag{1.6}$$

where the operator $\nabla = \nabla^*/L$ is used throughout and the body force term is scaled by the acceleration due to gravity. Selection of the characteristic scaling parameters is a bit of an art, but with care for a given scenario, if the scaling substitutions are $O(1)$ (i.e. normalized), then the relative weights of the terms can be analyzed directly through comparison of the relative magnitudes of the nondimensional parameters $St, Eu, Fr$, and $Re$:

[3]The viscous stress tensor, $\tau$, is hypothesized to depend on changes of velocity, whereby $\nabla \cdot \tau = \mu(\nabla\underline{u} + \nabla\underline{u}^T) = \mu\nabla^2\underline{u}$, with the volume viscosity taken as null.

$$[St]\frac{\partial \underline{u}^*}{\partial t^*} + (\underline{u}^* \cdot \nabla^*)\ \underline{u}^* \ = \ -[Eu]\nabla^* p^* + [\frac{1}{Fr^2}]\ \underline{g}^* + [\frac{1}{Re}]\ \nabla^{*2}\underline{u}^* \tag{1.7}$$

Viewed in this way, 'localness' can be determined in reference to the $\nabla^*$ operator. If changes in space of the field are on the order of the characteristic length of interest, then its effect is taken to be a local one. When the viscous forces of a given flow are much smaller than the inertial ones, the Reynolds number, $Re$, is large (i.e. $Re >> 1$), such that its reciprocal is small enough so as to neglect the final term of equation (1.7) outright. Where oscillating flow mechanisms are encountered, unsteadiness can be evaluated by the Strouhal number, $St$. When $St < 10^{-4}$, the contributions of the local accelerations are small and the fluid can be analyzed behaving as a steady flow. Corresponding considerations can be given to the Euler number, $Eu$, and the Froude number, $Fr$, for a particular scenario of interest.

## 1.3 More layers, thinner slices – a resolution problem

The physical processes of the lower strata which give rise to the microclimates therein are complex chiefly because the mixedness of the variables that characterize the system. Short and long wave radiation that determines surface heating distributions across domains of interest drive temperature gradients along the surface itself and the air above that may influence the relative humidity which, altogether, govern the average characteristics of a parcel of air swept away in a prevailing wind, issuing, say, from the mouth of a volcano, made visual to an observer by the mixed water vapor of the exhaust. In scenarios such as these, retaining a sense of scale is only made possible when held in reference to the subject of study. That is to say that the characteristics of the flyer (or particulate) and the objectives of the study themselves determine the scales that are appropriate to consider. Influences to the vicinity of the subject (i.e. its "local neighborhood") may of course derive from a scale much larger and slower, but the perceivable effects, from the view of the flyer, manifest only in an instantaneous and local sense. Thus, careful consideration is given to both the typical scales of the atmospheric processes in concert with the typical scales of the flyers themselves. Descriptions of the atmosphere over many horizontally extensive surfaces are oftentimes presented as spatial averages of vertical layers where sets of average properties are assigned to each layer division. Notions of layers and scaling are explored next.

**What are layers?**

The physical processes of transition from one state to another take place in layers. Horizontal layers, as adopted in this view, represent the transition from one state of a measurable set of parameters to another across sheets of material, with the flux across the boundaries oriented more or less vertically. The perception of change of a given domain demarcates the abutting boundary and the sharpness/gentleness of the transition determines the layer thickness. At the scales of interest here, regions [1] and [2] of fig. 1.1 will represent significant changes within and/or between microclimates, with special focus given to changes in wind. A microclimate as the term is used simply represents a local set of atmospheric conditions near the surface, characterized by moisture, temperature, and the parameters describing wind.

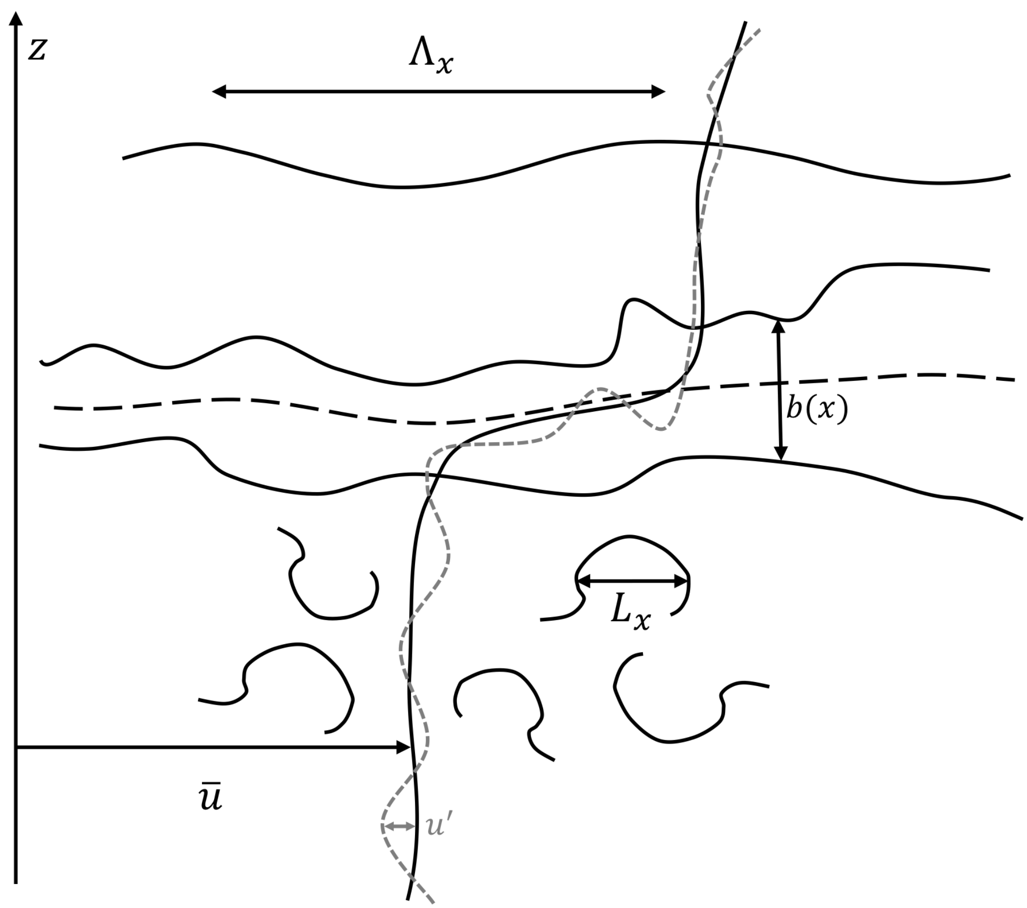


Figure 1.1: A conceptual view of a horizontal layer within a turbulent atmosphere characterized by superimposed quasi-coherent structures below and wave-like streamwise unsteadiness above.

**Layers in atmospheric boundary layer (ABL)**

Layers in the upper ABL establish differently in the daytime versus nighttime, on account of the drastic change in surface radiation, a consequence of the stability of the atmosphere to be discussed in more detail in a subsequent section. Figure 1.2 identifies the horizontal layers that comprise the ABL over an urban setting in day and night, a useful example that highlights the salient features of the more general ABL of any setting with relatively notable surface topography. The upper layers, denoted here as the mixed layer (ML) and entrainment zone (EZ), can be thought of as the initial gradation from free atmosphere down to the surface. In this region, which can occupy up to 90% of the ABL, atmospheric flux properties (e.g. momentum, sensible heat, water vapor) are nearly homogeneous with height due to the mixing effect of entraining less turbulent air down from the free atmosphere through the entrainment zone. Subgeostrophic wind in the middle portion of the mixed layer is nearly constant in speed and direction with turbulence in the region that is typically convectively-driven, though wind shear at the top of the mixed layer does contribute at times. The lowest $\sim$ 10% of the ABL is considered to be the surface layer (SL), which represents the most accessible region for measurements of all the atmospheric layers. The surface layer is comprised of an inertial sublayer (ISL) (present under specific conditions) and a roughness sublayer (RSL). Winds within the ISL at any instant vary randomly in space and are often described as stochastic- or continuous-gust velocity fields with an average wind speed profile observed to decrease with height nearly logarithmically to satisfy the no-slip condition at the surface. The RSL is the region where the flow is unequivocally influenced by the surface and the roughness elements upon it (if any). It is the RSL that is given special attention herein.

Subdividing further, but this time with vertical demarcations in either or both of the remaining directions, narrows the domain down to a column of air that may or may not vary in its thickness and/or extent. Such an abstraction, known as a control volume, may be arbitrarily assigned, or selected to contour about a given physical surface. Parameters fluxing across the boundaries of these defined spaces, when observable and repeatable, promote discovery of the physical laws that govern that particular volume of interest. The selected volume may represent a smaller part of a greater system or at most be the size of the greater system, but not any larger. This control volume view better emphasizes the so-called canopy layer (CL) as it cuts through a variety of microclimate domains, representative of a further horizontal subdivision of the RSL which generally connects the topmost features of roughness elements to their nearest neighbors, as illustrated in fig. 1.2. The salient features of three such representative microclimates will be highlighted next.

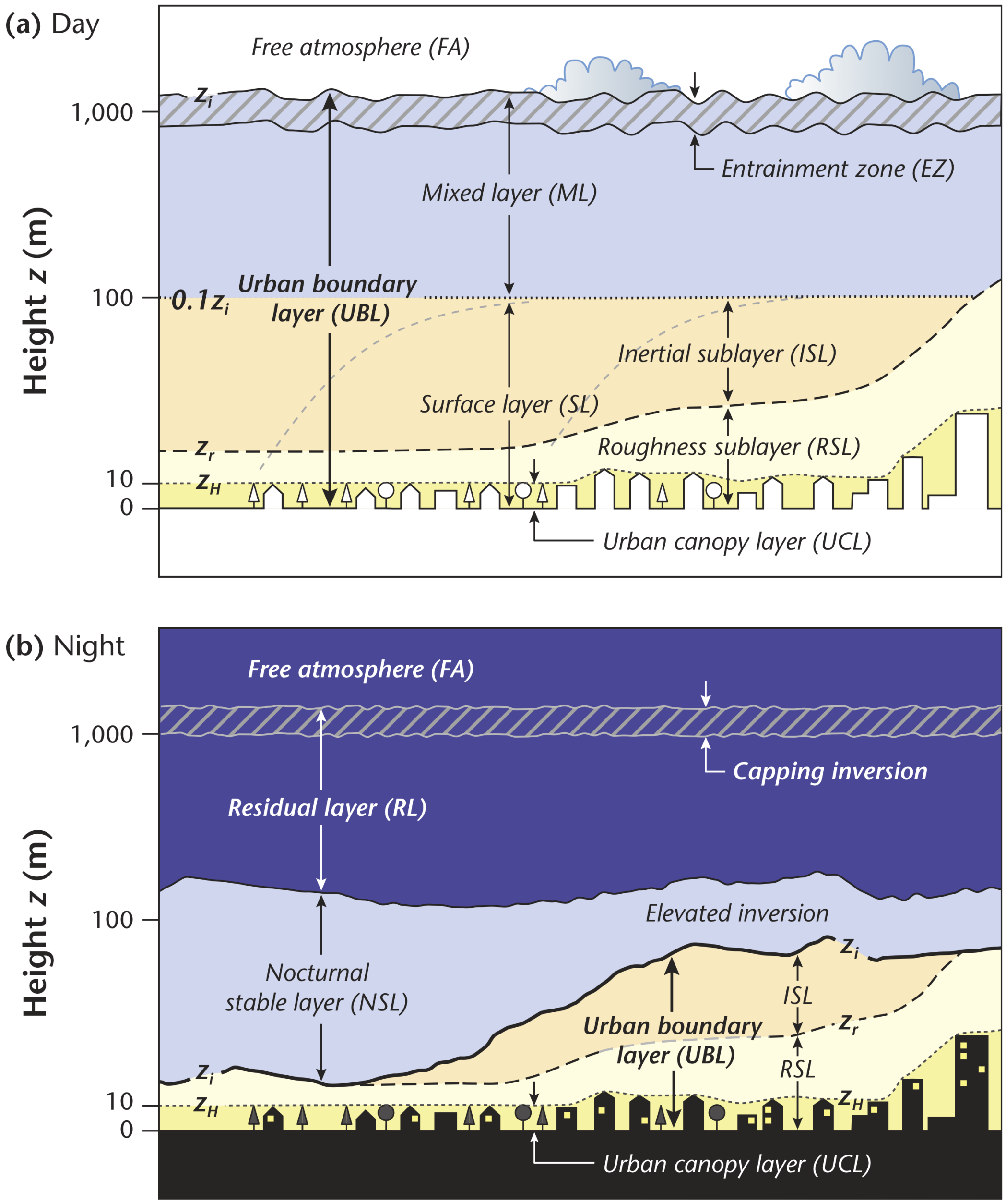


Figure 1.2: A view of the atmospheric boundary layer with its various sublayers established in (a) the daytime and (b) the nighttime. Figure reproduced from Timothy R Oke et al. (2017) with permission of Cambridge University Press through PLSclear.

## 1.4 Touring the various microclimates

With a better understanding of the physical mechanisms that drive the complex dynamics of the ABL now established, three representative microclimates will be explored to further elucidate the relevant fluid events a flyer may experience near the surface. Though outside the scope of current experimental work, as full of an environmental description (i.e. moisture, temperature, and wind) is given as possible, prior to ultimately reducing the scope to a neutrally stable atmosphere above a canopied surface devoid of any major weather events other than a reasonably strong prevailing wind. Building an intuition for the environmental domains of interest will serve as a reminder of the interconnectedness of the local set of atmospheric conditions that ultimately contribute to shaping the local nature of the wind and how it behaves upon encountering surface roughness elements.

### The urban microclimate

Built-up manmade structures of various heights clustered pseudo-randomly upon a location of mixed surface cover where heat, water, and various pollutants are exchanged into the atmosphere well-describes an urban microclimate. Flow among and between buildings and the subsequent turbulent wakes produced are prevalent and generate eddy sizes dependent on the geometry of the roughness element, angle of incidence, and its shedding process. The urban canopy layer (UCL) is defined by the ground below and a contoured boundary connecting building tops above, as drawn in fig. 1.2. The effects of the presence of the UCL can be felt upwards of two to three times the average building height, featuring large variability in the mean and turbulence flowfield properties. Turbulence within this region is characterized by increased vertical momentum flux on account of the increased mechanical turbulent mixing from obstacle wakes. A maximum value of turbulence kinetic energy is found to occur somewhere between just above roof height and twice the building height. Due to the intense mixing right above and the wake production amongst and between buildings, typical similarity scaling methods[4] used in the upper portions of the ABL do not apply in the urban canopy layer (Christen et al., 2007; Roth, 2000).

[4]For example, the Monin-Obukhov similarity theory (MOST) for the subinertial range of the ABL assumes an approximately constant turbulent flux density of heat, mass, and momentum with height as well as the typical assumptions of homogeneity and stationarity of turbulence for closure of the turbulent boundary layer equations.

Figure 1.3: The local cityscape of 53rd and Park Avenue in New York City, NY, centered upon Seagram building and plaza. Not only must a flyer contend with the effect that heterogeneity of the manmade-building cityscape has on local winds, but also on the environmentally-driven factors of its location in Midtown Manhattan, an island bounded by the Hudson river to the west and the East and Harlem rivers to the east.

**The vegetation microclimate**

Consider next a plant cover, like a forest, that occupies space between the surface and the atmosphere. Radiative processes are absorbed and reflected like solid boundaries on the various leaf, branch, trunk surfaces but the remainder light can pass through and air motions can circulate beneath and within. The finite thickness layer formed that divides the under-canopy from the above-canopy of tall vegetation represents a permeable and living layer that photosynthesizes, respires, sheds, and grows with the shifting seasons. Temperature differentials from sun to shade and water vapor distributions can both change on account of the winds. Gusts or sweeps can usher in sudden inflows of the atmosphere above to the understory below whereas bursts or ejections have the opposite effect. In a forest with profuse foliage but a clear trunk space free of thickets and sapling growth, winds speeds in the under-canopy may exceed those of the crown, but do not (typically) exceed wind speeds in the above-canopy on account of the aerodynamic drag on the plants. An inflection point in the mean velocity profile is oftentimes observed at the top of the plant canopy layer (PCL) (Raupach et al., 1996), initiating the eddy diffusion processes that more efficiently exchange air masses. Canopy turbulence intensities are far higher than anywhere else in the surface layer on account of energy production in the intense shear layer at the plant tops, though smaller scale turbulence produced from plant wakes contribute too. Due to the spatio-temporal complexity of turbulence in the PCL, combined with the sinks-and-sources of momentum and scalars alike, typical similarity scaling methods used in the upper portions of the ABL do not apply in the PCL (Kaimal and J. J. Finnigan, 1994).

Figure 1.4: A gridded agricultural canopy of date palm trees (Thermal, CA). In this view, relatively slender trunks uphold rather large canopy crowns that demarcate the atmosphere above from the under-canopy below.

**The mountain cliffside - Mars**

Finally, consider exploration of the Red Planet through the eyes of the Rover. No buildings or trees to be spotted, but cliffscapes can be made out when the dust settles. Daytime is stark in comparison to night. Along the Rover wheels, the ground temperature may be 15K higher than at its tallest mast, a mere six feet above, only to plummet an extra 100K when night arrives to switch the gradient direction. Both the short wave radiation of the sun and the long wave absorption by the CO2 contribute to large horizontal temperature gradients from mountains to plains to craters that drive topographically-induced thermal circulations during the day. The resulting convective motions may swirl up a dry and wandering dust devil (Schofield et al., 1997) or katabatic winds down the crater slopes and into the dune fields. The atmosphere is thin, about 1/100th the density that its earthly twin and water is scarce, thousands of times less precipitable than an equivalent Earth atmospheric column (Jakosky and Phillips, 2001; Smith et al., 2001). Due to the intense radiative heating-cooling cycle, typical similarity scaling methods used in the upper portions of the ABL do not apply in the Mars planetary boundary layer (PBL) near the surface.

Figure 1.5: Hillside outcrop within Murray Buttes region, lower Mount Sharp. Images taken by MASTCAM onboard NASA's Mars rover Curiosity on Sol 1419 and processed further by Seán Doran (NASA et al., 2016), use under: CC BY-NC-ND 2.0.

## 1.5 Wind near the surface

In general, air motions observed to vary randomly in space and time subject to the stability characteristics of the atmosphere at a given location, when averaged, are reported as a horizontal wind speed $u_h = \sqrt{\overline{u}^2 + \overline{v}^2}$ oriented in a certain compass-based direction, a safe assumption when the average vertical wind component $\overline{w}$ is much smaller than the horizontal wind components $\overline{u}$ and $\overline{v}$, as is often the case in the surface layer. By aligning our view with this prevailing wind, and when averaging over homogeneous horizontal layers, conceptually, a two- or potentially three-dimensional mean velocity field can be evaluated as a one-dimensional (assuming divergence is small) horizontal wind that varies with height $z$. Winds "near the surface", which is oftentimes meant synonymously to flowfields within the RSL in this dissertation, can be made more explicit by considering a bounding height parameter beneath which dynamic turbulence (i.e. mechanically-driven) dominates, a concept explored next.

### Stability of winds - time of flight

A measure of the stability of the atmosphere in relation to the isentropic motion of a fluid particle due to the temperature gradient in a stationary atmosphere was previously discussed but can further be identified circumstantially by the characteristics of air motions during specific times-of-day. For instance, at night as the surface radiatively cools outward toward space, lighter-warmer air from above moves downward toward the surface, tending to suppress the vertical displacements of fluid elements. This negative buoyancy flux associated with the positive temperature gradient describes a stable atmosphere and if winds in the region are particularly weak, one may add select descriptors to mark its relative stillness. Classifications of stability, when reported, are often done so rather qualitatively (e.g. "strong", "moderate", "weak", "very weak" in the Turner Classes Turner, 1964), in large part because meteorologists rarely know the actual local gradients[5]called for in the turbulence kinetic energy equation. For the purposes herein, measures of stability (i.e. how a fluid particle may behave when put into vertical motion against the backdrop of time-averaged local conditions) simply act as broad indicators of the likelihood and prevalence of turbulence in a region at a given altitude for a given time-of-day, couched in the understanding that even statically stable air can be made to create turbulence dynamically through wind shear in the surface layer. As such, because the energetic overlaps of the forcing spectrum and the natural modes of the flyers predominantly occur in the high-frequency turbulent fluctuations portion of the spectrum, the turbulence of note when testing the response characteristics of flyers of interest will almost always be mechanically-driven.

The Richardson number ($Ri$), a measure of the relative magnitudes of shear (mechanical) production to buoyant consumption in the turbulence kinetic energy equations, can be used to signal when a flow may become dynamically unstable. For example, when $Ri > 0$, layer stratification is stable and the development of turbulence is hindered[6]. When the $Ri < 0$, with temperature gradients superadiabatic, layer stratification is unstable and the intensity of turbulence increases. At $Ri = 0$, temperature distribution with height is adiabatic, the layers are neutrally-stratified and the turbulent processes occurring within are strictly mechanically-driven. Though useful in its various forms in meteorology, the Richardson number says nothing to the intensity of turbulence likely to be experienced by a flyer flying through, and only expresses the tendency of a flow to become or remain turbulent (or become and remain laminar). Because the value of $Ri$ approaches zero near ground level (no-slip), evidently a sub-layer exists where the influence of stratification due to a given temperature distribution in an inhomogeneous atmosphere (whether stable or unstable) is small enough to neglect, and a *near-neutral* stability condition is reasonably met. By extending criterion to diabatic (non-neutral) environments through a correction factor that accounts for the buoyancy contributions, Obukhov derived a conditional length characteristic $L_O$ he called "the height of the sub-layer of dynamic turbulence", which is typically on the order of tens to hundreds of meters and varies diurnally, even in fair weather conditions (e.g., see Stull, 1988, Fig. 5.21), given here as

$$L_O = \frac{-u_*^3 \overline{\theta}_v}{\kappa g (\overline{w' \theta_v'})_o} \tag{1.8}$$

where $\overline{\theta}_v$ is the mean virtual potential temperature and $(\overline{w' \theta_v'})_o$ is the virtual potential temperature flux at the surface. The physical interpretation of the Obukhov length as a height *proportional* to which the buoyant production of turbulence dominates the mechanical production of turbulence is a useful bounding parameter for the purposes herein. For instance, when $L_O < 0$ (indicating an unstable atmosphere, typical on sunny days due to convective heating), $|L_O|/10$ can be taken as the height that

[5] Approximations of these gradients via more readily available observations do provide more quantitative metrics, such as the NOAA GOES-R Series Advanced Baseline Imager (ABI) Level 2 Derived Stability Indices (DSI).

[6] In theory, beyond a certain critical $Ri$, turbulence can be suppressed outright.

separates the predominantly mechanical from predominantly convective turbulence (Panofsky, 1984). A dimensionless height $\xi$[7]based on the Obukhov length provides the most utility, as the sign of $\xi = z/L_O$ implies the stability of the atmosphere in the surface layer and the magnitude of $L_O$ determines the altitudes $z$ at which dynamic turbulence is expected to dominate. Though we acknowledge the effects of atmospheric stability in the upper layers of the ABL, winds near the surface characterized by predominant mechanical turbulence will be treated as satisfying (even if approximate) a near-neutral condition. This focus on reasonably strong winds ensures near-neutral conditions are essentially always met so that $L_O \to \infty$.

**Wind profiles**

In the upper regions of the surface layer, the influence of individual surface features reduces to the point where their roughness can be accounted for in an integral sense. That is to say that when considering *mean* characteristics of the velocity field in the inertial sublayer (ISL) in a neutrally-stratified atmosphere, the spatial variability of atmospheric properties introduced at or near the surface are sufficiently homogenized so as to be considered akin to a sandpaper roughness in the canonical turbulent boundary layer studies of flows over smooth and rough surfaces, as first suggested by Prandtl (1932). The logarithmic law of the wall, put forth by Kármán (1931), and adjusted for surface roughness can be given as:

$$\frac{\overline{u}_h(z)}{u_*} = \frac{1}{\kappa} \ln\left(\frac{z - z_d}{z_0}\right) \tag{1.9}$$

where $u_*$ is the friction velocity ($\sqrt{\tau/\rho}$), $z_d$ is the zero-plane displacement thickness that moves up the height of the effective uniformly-rough surface 'felt' by the flow, $z_0$ is the roughness length typically found through extrapolation of $\overline{u}_h$ to zero, and $\kappa \approx 0.4$ is von Kármán's constant. The zero-plane displacement thickness included in eq. (1.9) reflects the reality that momentum is absorbed predominantly by the upper portion of the canopy roughness elements. A so-called exponential wind law was formulated by Cionco (1965) for flow within an 'ideal' vegetation canopy (i.e. uniform geometry and distribution) and was later modified by Macdonald (2000) in wind tunnel studies of arrays of bluff elements (cubes with height $H$) to more closely represent the features of an urban-type surface. Through an empirically-determined attenuation coefficient (that can be related to the turbulence length scale), spatially

[7]A functional dependence on this dimensionless height forms the premise of the so-called Monin-Obukhov similarity theory (MOST), applicable to the profile equations in the constant-flux portion of the surface layer, valid $|\xi| < 1 - 2$. Foken (2006) notes that even in ideal conditions over homogeneous surfaces, MOST is only about 10-20% accurate.

averaged velocity profiles within the canopy ($z < z_H$) were modeled as:

$$\frac{\langle \overline{u}_h(z) \rangle}{\langle \overline{u}_h(z_H) \rangle} = \exp\left[a\left(\frac{z}{z_c} - 1\right)\right] \tag{1.10}$$

where $z_H$ represents the measurement location at $z = H$ and $a$ is the attenuation coefficient found to be $a = 9.6$ for in-line and staggered arrays of cubes of uniform height. Christen (2005) found adequate agreement for the exponential decay law of eq. (1.10) within the upper portion of an urban canopy layer based on extensive field site testing, whereas Castro et al. (2006) noted its deficiency in higher density roughness cube distributions in wind tunnel studies. Florens et al. (2013) suggest a linear in-canopy velocity profile from measurements with a high resolution PIV system. More to the point, whatever shape the velocity profile within the canopy layer may take, an inflection point of the mean velocity profile is noted to occur near canopy height $z_H$ in every study of wind flowing across the face of roughness elements (the implications of which will be discussed in a subsequent section). When taken together, wind profiles in the surface layer above distinct canopies can be roughly represented as in fig. 1.6, with the discrepancies of in-canopy velocity profiles noted as above.

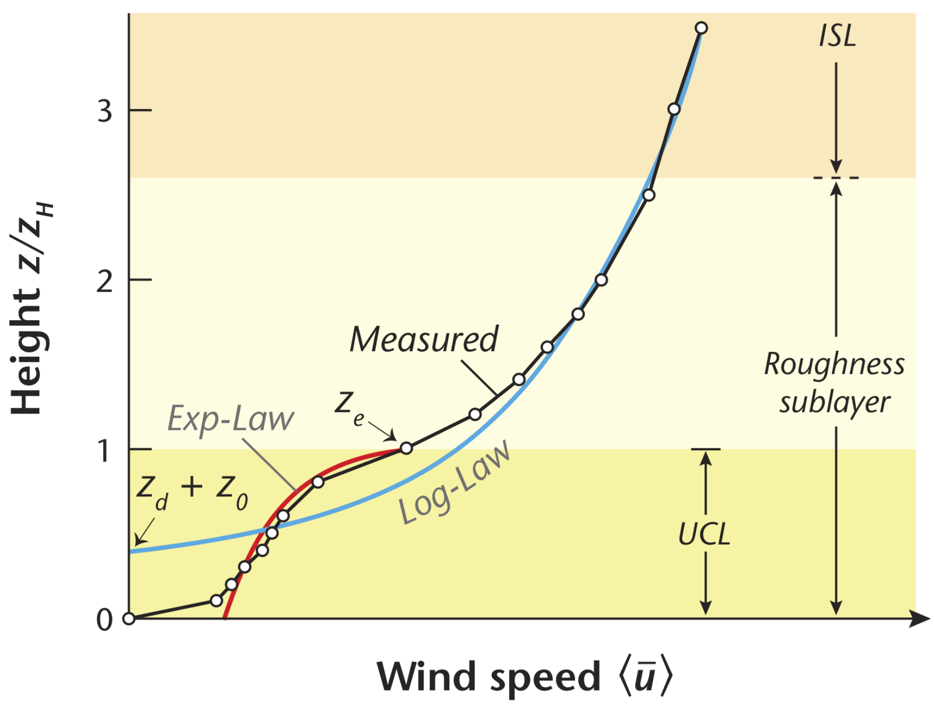


Figure 1.6: Wind profile with the log-law (eq. (1.9)) and exp-law (eq. (1.10)) included for comparison against the demarcated surface layer of fig. 1.2a. Figure reproduced from Timothy R Oke et al. (2017) with permission of Cambridge University Press through PLSclear.

**The nature of the winds near the surface**

The wind profiles presented in the previous section, though useful mathematical constructs, obscure the true instantaneous nature of winds which are nearly always turbulent and unsteady. Because atmospheric motions occur over a huge range of temporal and spatial scales, it is useful to know how the energy of the atmosphere at a location distributes amongst those scales. Perhaps the most direct view is that of the spectrum. In general, a spectrum plotted for an atmospheric quantity measures the distribution of the variance of that given variable in relation to frequencies or eddy sizes. When the variable in question is a time record of a velocity component, the spectrum then describes directly the distribution of (kinetic) energy with respect to frequency. The kinetic energy of horizontal air motions within the atmospheric boundary layer under certain conditions is observed through field experiments (see Davenport, 1961; Van der Hoven, 1957) to distribute into two distinct energy bands with a gap in between.

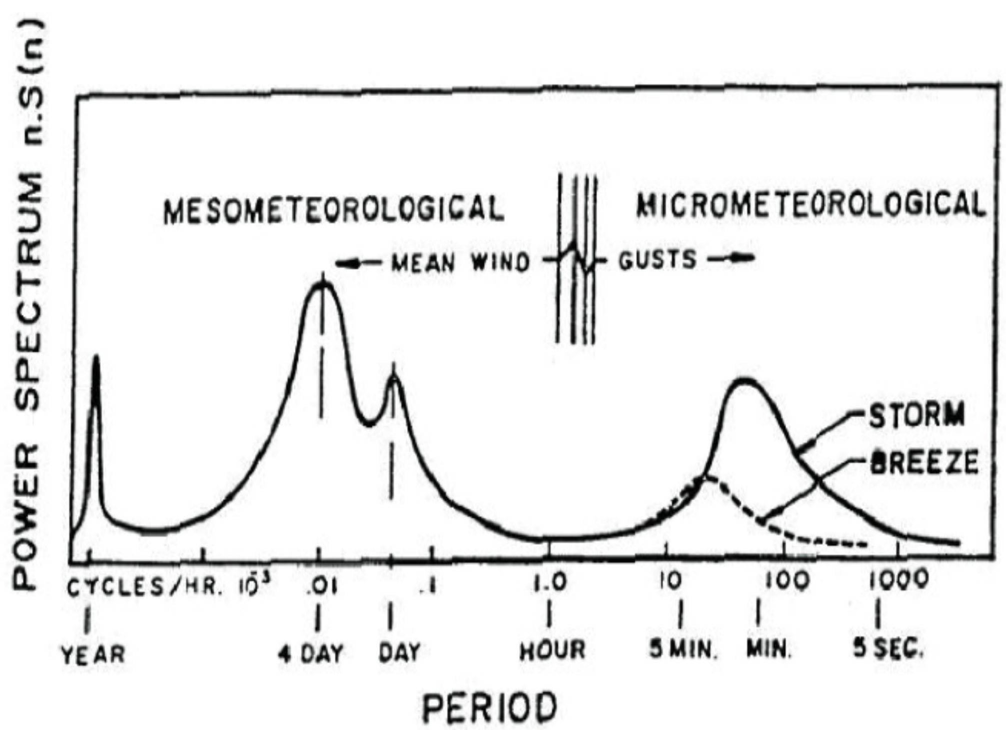


Figure 1.7: Evidence of the spectral gap from the Van der Hoven spectrum at the Brookhaven site from two occasions, one in nominal conditions ('breeze') and the other purposefully tested during hurricane Connie ('storm'). Figure republished with permission of Springer, from Stathopoulos and Baniotopoulos (2007), after Van der Hoven (1957); permission conveyed through Copyright Clearance Center, Inc.

Synoptic scale instabilities associated with horizontal wind gradients create large-scale (horizontal) atmospheric motions on the order of several thousand kilometers, representative of the types of macroscale atmospheric flow systems that can be resolved on weather maps. In contrast, microscale motions representing fluctuations with periods less than about one hour occur predominantly due to heating and the frictional motions of air near the surface. Sitting inbetween are the mesoscale motions that account for strong diurnal variations such as sea breezes and gravity waves.

When energy distributes amongst specific energetic bands, advantages in analysis emerge; chief among those are the treatment of those particular frequency bands as statistically independent of estimates in other frequency bands. Power-spectrum analysis of horizontal winds in the ABL suggests a major energetic peak at a period of nearly four days (corresponding to fluctuations in wind-speed driven by the passage of large pressure systems) and a second discernible spectral peak at a period of about one minute (the average time from one gust to the next on account of the convective and mechanical turbulent fluctuations). Separating the two is a broad and, at times, consistently low-amplitude energetic lull centered upon periods approximately ranging from ten minutes to an hour. J. Lumley et al. (1964) suggest that in order to discuss the statistical properties of microscale turbulence in the ABL in isolation from the larger scale turbulence it is embedded in, a spectral gap is necessary. When held in reference to the flyers of interest, the existence of a statistically significant spectral gap is of secondary importance compared to the energetic bands overlapping the representative time and length scales of the flyers themselves, as will be discussed in section 1.5 However, justification in the analysis of winds in the ABL through a decomposition of the instantaneous velocity field hinges upon the suitable separation of such scales, where the synoptic scale peak is said to be associated with the *mean* flow and the microscale peak associated with *stochastic gusts*. The stability of the atmosphere at a particular location ultimately determines the nature of the microscale motions (i.e. the size and frequency) likely to be encountered by the near-surface flyer but because the mechanical turbulence tends to increase with the square of wind speed, the contribution of convective turbulence will always be comparatively small in the presence of a reasonably strong wind, validating the likelihood of a spectral gap in strong wind conditions and further diminishing the influence of stratification in these studies.

**The scales of and within the surface layer**

Response characteristics of a flyer flying through the surface layer depend directly on the forcing spectrum of the environment, and a particularly strong amplitudinal-response would occur at frequencies where energy in the forcing spectrum coincides with flight dynamic natural modes[8]. For the flyers of interest herein, natural modes are typically on the order of $10^0$ cycles per second (Hz) (and sometimes even upwards of order $10^2$ Hz), such that overlap in the forcing spectrum would nearly always occur in the microscale portion of the spectrum. As such, the mean wind motions in the surface layer averaged over 30-minute time histories or modeled by eq. (1.9) and eq. (1.10) and assigned as descriptors of the synoptic scale motions are of secondary importance when held in comparison to the fluctuations of and about the prevailing winds of the region where the flyer will fly, as it is flying. This pushes towards a more intimate understanding of the microclimatogy of the region (as was explored previously) at a given time-of-day amongst the backdrop of the local terrain, because ultimately the statistical structure of the microscale motions is determined by the wind speed, the atmospheric stability, and the terrain characteristics. Coupled with the variability in flyer design, it is rather unlikely to account for every scenario in a single diagram. Instead we choose **an urban cityscape as a model environment** as it represents some of the tallest, bluffest, and most heterogeneous of the canopied topographies, further enriched and complicated by the imprint of humankind. Figure 1.8 showcases the order of magnitude overlay of characteristic flyer time and length scales compared to example urban (micro)climate phenomena in a standard time-space plot. Length and time scales of interest are defined and noted as intuitively as possible. Consistent with the bulk of literature in the atmospheric sciences, micro- here does not indicate scales of the order $10^{-6}$, but rather a smaller complement of a broader, more macro- view. For instance, as put forward by Sutton (1953) micrometeorology denotes “the intimate study of physical phenomena taking place over limited regions of the surface..., and usually within the lowest layers of the atmosphere”, which is held in contrast to the synoptic-scale weather systems that involve large regions of great depths. The same applies in the microclimate and (macro-)climate complement. Many such naming conventions exist, highlighting the difficulty in grouping processes that at any instant or at a particular place may not actually conform to its assigned subdivision. For

[8]It is customary when modeling the effects of turbulence in design studies for manmade flyers to summarize the effects of system dynamics by treating the (linearized) spectral response of a flyer as a product of the forcing spectrum and its transfer function.

this reason, where possible, ellipsoids are drawn to better represent the variability inherent to the domains of interest as they present across broadly-encompassed fields of study.

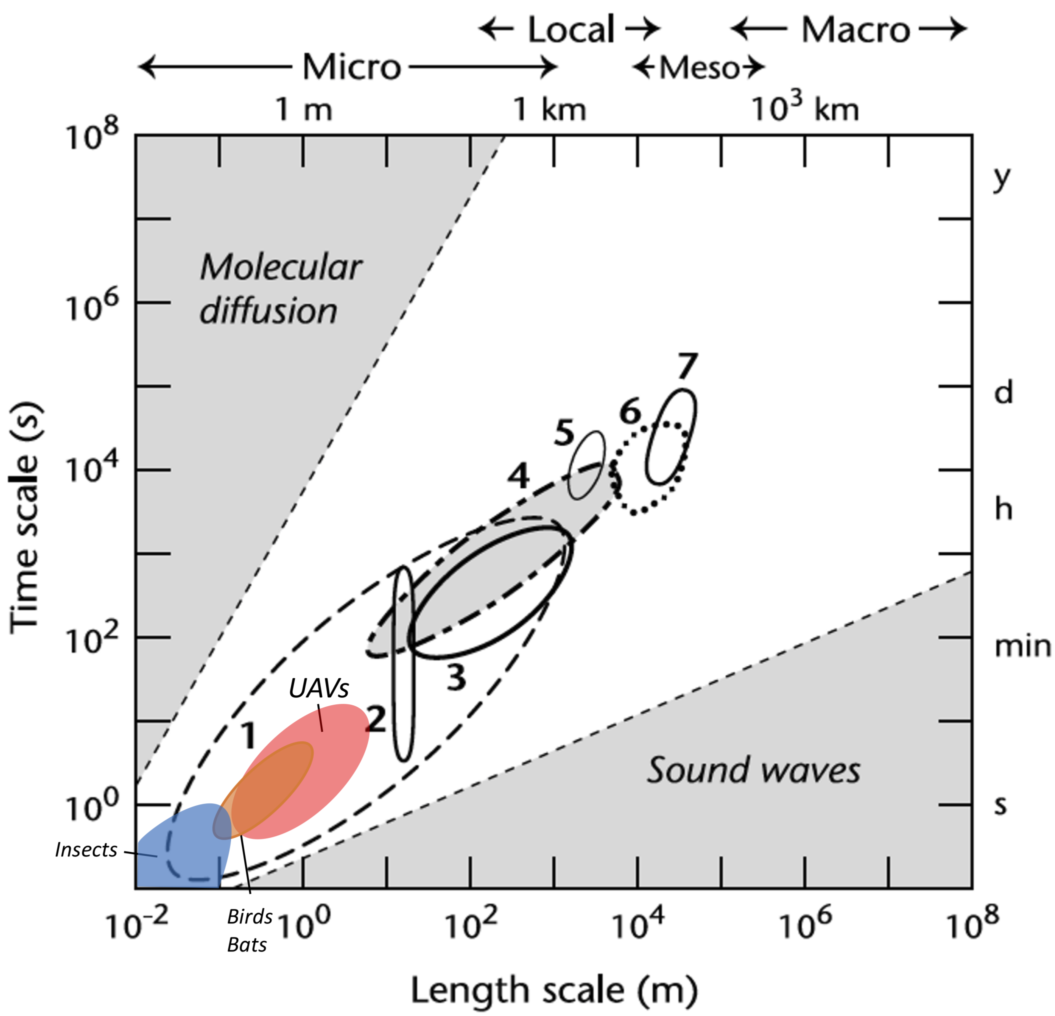


Figure 1.8: The conventional atmospheric length scales of macro-, meso-, local-, and micro- are defined atop and put into urban cityscape reference elements below. Characteristic time scales are given at left and put into colloquial divisions at right. It is interesting to note the separation of scales between the flyers (UAVs, birds, bats, insects) and the majority of likely urban atmospheric fluid events. Overlap in the dashed region 1 corresponds to mechanical eddies shed by obstacles. 2 - cross-canyon vortex; 3 - individual building wake; 4 - chimney stack plume; 5 - urban park breeze circulation 6 - urban-rural breeze system; 7 - uplift in city ‘plume’. Figure republished and modified with permission of Springer Nature BV, from Tim R Oke (2006); permission conveyed through Copyright Clearance Center, Inc.

## 1.6 Treatment of flows near the surface: a simplified view

Though the focus of this dissertation remains extensibly on the exposition into simulation techniques for the three flow regimes directly above, at, and within the canopy layer (CL) embedded within the roughness sublayer (RSL), a quick departure up to the inertial sublayer (ISL) is warranted, if nothing more, by the simple fact that the majority of available field study data and the bulk of modeling efforts has focused on treatment of roughness at the surface as a homogenous porous medium. With but few exceptions, many of the tower measurements to be referenced subsequently would describe the terrain of measurement as an open field (e.g. farmland, grassland, desert) broken only by a few trees, some hedgerow, or distant structures, each in their own way far from the environment of the built-up urban cityscape selected as a model for consideration herein. The modeling of atmospheric turbulence far above cities or near airports (or any other take-off and landing locations), however, is well-established and an important consideration for the handling characteristics and structural integrity of the larger-faster flyers that ascend/descend through the surface layer up-to/down-from cruising altitudes far outside the local microclimate views considered thus far. Even though peak energies in the forcing spectrum of the disturbance environment far from local effects do not overlap the frequency regimes of the smaller surface-bound flyers of interest herein, a discussion and simulation technique for the microscale motions in the ISL is included for completeness to complement the more local considerations in the RSL to follow.

### Treatment of flows within the inertial sublayer (ISL)

The universality of wind motions in the inertial subrange over 'rough' walls is well-established provided the surface roughness height remains below a certain threshold relative to the boundary layer thickness. Jiménez (2004) suggests that if the height of the roughness element at the surface does not exceed 2-3%[9] of the boundary layer depth $\delta_{BL}$ (typically cited as $\sim$ 500m for the near-neutral atmospheric boundary layer), the most important effect of roughness is the change of mean velocity profile near the surface. Time-averaged statistics in the atmospheric surface layer far from local effects can generally be accounted for by the Monin-Obukhov similarity theory (MOST), which proposes universal functions that scale height $z$ with the Obukhov length $L_O$. In the presence of strong winds in a neutrally-stratified atmosphere ($L_O \rightarrow \infty$), the mean velocity profile in the windward direction reduces to the familiar logarithmic law of the wall of the canonical turbulent boundary layer, presented in section 1.5, so that when adopting a more global view and considering flight within the ISL (say, $z \approx 3H$) above short roughness elements with average geometric height $H$ that do not constitute a canopy, differences in terrain roughness can safely be accounted for by use of a bulk surface roughness parameter, such as the roughness height $z_0$.

To center the conversation, consider a flyer attempting to maintain its hover position in the presence of a continuously-gusting velocity field high above a city or somewhere in an open field. In this coordinate system (averaged over homogenous horizontal layers), since the flyer neither appreciably gains nor loses altitude, the velocity field experienced will change in time but not in space, with peak spectral energy of the environmental disturbances occurring typically with a period of one minute or so, in accordance with observation such as in fig. 1.7. For typical gusting velocities approaching $10^1$ m/s, associated longitudinal distances between wavefronts in a horizontal wind would then be of order $10^2$ m for a spectral peak at a period of one minute, about one or two orders of magnitude greater than any typical geometric dimension of the flyers of interest, according to fig. 1.8. It does not appear, then, that any specific length-coupling in the longitudinal direction emerges when considering stochastic gusts in the surface layer far enough from the specific wavelengths introduced by the geometries of the roughness elements at the surface, such that the flowfield is experienced globally from the perspective of the flyer. Atmospheric turbulence in the inertial sublayer (ISL) is observed to essentially behave isotropically, analogous to the inertial subrange in the canonical turbulent boundary layer of smooth and rough walls, where eddies with no obvious direction-preference transfer energy without loss from the larger scales down to the smaller scales.

### Modeling the form of the spectrum far from local effects

Davenport (1961) compiled horizontal wind velocity records when mean velocities exceeded 9 m/s, all measured below $z$ = 150 m at three different tower sites. He proposed a form of the spectrum[10]to fit observation based on the assumption that the energy of the eddies should be proportional to surface drag (and therefore the square of the mean velocity) measured at some reference point near the ground. The drag coefficient is more commonly used in the wind loading of structures but can be related to the roughness height $z_0$ (see Wieringa, 1992). Though empirical fits to observed data can be useful for some engineering models, the lack of theoretical basis

[9]Amir and Castro (2011) and Florens et al. (2013) provide some evidence that number may be closer to 7%.

limits its scope, particularly for analyses that depend on the shape of the spectrum. On strictly theoretical grounds, Kármán and Howarth (1938) calculated correlation coefficients for two arbitrary velocity components for isotropic turbulence. By considering the Fourier transform of these correlation functions, Kármán (1948) showed that, for large Reynolds numbers, the shape of the spectral function would be proportional to $k^{-5/3}$ when $k$ is large, and behaves according to $k^4$ for small values of $k$, where $k = 2\pi f/\overline{u}$ is the wave number of the fluctuation and $\overline{u}$ is the mean horizontal wind speed. The interpolation formula that was proposed by von Kármán was adapted for the case of fixed-wing airplane response to continuous random atmospheric turbulence in Diederich and Drischler (1957). Its use in flight applications is well summarized in Etkin (1981), and for helicopters specifically in Gaonkar (2008). The power spectral density of the longitudinal component of the velocity field, based on von Kármán's atmospheric turbulence formulation, is then written as:

$$\Phi_u(\omega) = \frac{2\sigma_u^2 L_u}{\pi V} \frac{1}{(1 + (1.339\frac{L_u \omega}{V})^2)^{5/6}} \tag{1.11}$$

where $\omega = 2\pi f$ and $V$ is the simulated flyer speed. Two parameterizations are required in this formulation, namely the turbulence scale length $L_u$ (assumed to be $\sim 750$ m when unknown) and the root-mean-square (R.M.S) of the fluctuations $\sigma_u = (\overline{u'}^2)^{1/2}$, which can be derived from the intensity of the random turbulent motions in the ABL (i.e. $TI_u = u'/\overline{u}$) known to vary with altitude and range from $5 - 30\%$. Measurements taken in the ABL near the surface away from local topographical effects during convectively stable and mixed atmospheres suggest integral length scales $L_u$ to be on the order of the flyer altitude (Witte et al., 2017; Yeung et al., 2018), though calculations for this particular turbulence length scale have long been challenging and should be interpreted with caution due to the non-stationary behavior of winds near the surface. Here, Taylor's frozen turbulence hypothesis used

[10]Because there appeared to be only slight variation in the strong horizontal wind spectrums with height, no characteristic length for the horizontal components of gustiness that depended on altitude or surface roughness length could be identified, and was instead taken as constant to render an (empirical) expression for the spectrum of gustiness in strong winds in the lower layers near the surface but far from local effects to be:

$$\frac{f \cdot E_{11}(f)}{\varkappa U_{10}^2} = 4.0 \frac{s^2}{(1 + s^2)^{4/3}}$$

where $U_{10}$ is the reference mean velocity measured at $z = 10$ m, $\varkappa$ is the drag coefficient, and $s = 1200 \cdot f/U_{10}$.

in conversion from the frequency domain to the wavenumber domain is doubtful to apply, since a single constant convective velocity describing all frequency scales is not readily apparent as mean wind speeds change over time. Due to the potential of 'smearing' in the spectral analysis in wavenumber space, it is recommended that classification of large-scale structures in the atmospheric surface layer be carried out in the frequency domain when mean wind speeds change appreciably according to measured temporal wind records (Guala et al., 2011). Velocity fields with significant non-stationary behavior will be presented in the frequency domain only. When comparing to Kármán's form of the spectrum, $L_u$ will be assumed order of magnitude of the altitude at which the turbulence intensity is specified.

The theoretically-derived $-5/3$ power law behavior of the microscale structure of turbulence is observed to occur in the inertial sublayer (ISL) both from measurements on instrumented aircraft (Sheih et al., 1971; Witte et al., 2017) as well as from tower measurements far from topographical influences (Pond et al., 1963; Watkins et al., 2010). This region typically spans three decades of frequencies in a neutrally-stable atmosphere with the Reynolds number based on the root-mean-square of the fluctuating component $u'$ and $\lambda_T$ (i.e. $Re_{\lambda_T} = u'\lambda_T/\nu$) ranging from 2880 to 5330. The so-called Taylor microscale $\lambda_T$ is a characteristic length scale commonly used in isotropic turbulence to denote an intermediate size eddy that is smaller than the larger energy-accepting eddies but larger than the dissipative eddy scales. This forms the basis of the preferred atmospheric disturbance model required by the military (MIL-STD-1797A) and the Federal Aviation Administration (FAA, part 25, appendix G) to model the flying qualities of a piloted fixed-wing aircraft in the ABL because it properly resolves the effects of structural modes at higher frequencies. The model relies on airplane motion through the spatially-varying continuous gust field to generate temporal variations in wind velocity ('frozen in time') and thus excludes its use in hover applications.

**Treatment of flows within the roughness sublayer (RSL)**

Close to rough surfaces, the Monin-Obukhov similarity theory (MOST) no longer holds. Turbulent fluxes near plant canopies or urban areas are nearly always greater than is predicted by MOST from observed mean gradients on account of the change in the dominant flow mechanism of turbulence generation due to the presence of coherent structures. Consider a prevailing wind flowing left to right relative to the viewer for each of the frames of figs. 1.3 to 1.5, with a control volume fitted exactly to the frame. Due to the occurrence of intermittent coherent structures within the specified control volume, traditional boundary layer scaling techniques ultimately fail. These coherent structures are initiated by Kelvin-Helmholtz instabilities, that unlike their gentler counterparts (e.g. gravity-waves on a cool night) roll up into coherent vortices before ultimately breaking down into turbulence. This process initiates vigorous turbulent exchange of the properties of the air masses above-and-below or from within-and-without. Conceptually, moving across the interface of the dividing streamline (be it urban, vegetation, or cliffside) is characterized by notable velocity gradients, the steepness of which coupled with the angle of entry determining the closest analogous forcing input experienced by the flyer passing through. The region into which the flyer enters would vary dependent upon the morphology of the roughness, thus further shaping the forcing input experienced by the flyer.

### The roughness sublayer immediately above and below the canopy eddies

Recognizing that there is at least one more relevant length scale within the roughness sublayer, a simple coupled canopy-surface layer model analogous to MOST that scales additionally with $\delta_\omega$ was developed by Harman and J. J. Finnigan (2007) and for neutral-conditions by Poggi et al. (2004) scaled with the geometric roughness element width $d_r$. Poggi et al. (2004) notes that for a regular array of vertical rods, at least near $z \approx H$, dense canopies share many attributes with perturbed mixing layers. At an altitude within the roughness sublayer (say, $z \approx 1.25H$) above the location of the inflection point near the canopy top ($z \approx H$), a longitudinal length scale associated with the dominant flow mechanism of the coherent structures must also be considered. One candidate is the streamwise separation $\Lambda_x$ of the coherent structures themselves, observed to be approximately four times the shear layer width $\delta_\omega$ at plant canopy tops (Raupach et al., 1996), well within the range observed for planar mixing layers generated in the lab (see Dimotakis and Brown, 1976). The specific details of the coherent structures at the canopy top (i.e. $\delta_\omega$ at $z \approx H$) are rarely reported and the longitudinal length scale from correlation data $L_x$ measured away from the canopy eddies is often given in ratio to the more readily available geometric roughness element height $H$.

[10] Orographically-induced turbulence (e.g. gravity-waves) wouldn't be fast enough ($St \sim 10^{-2}$) to compete with the quasi-periodic eddies ($St \sim 10^{0}$) at the canopy layer boundary.

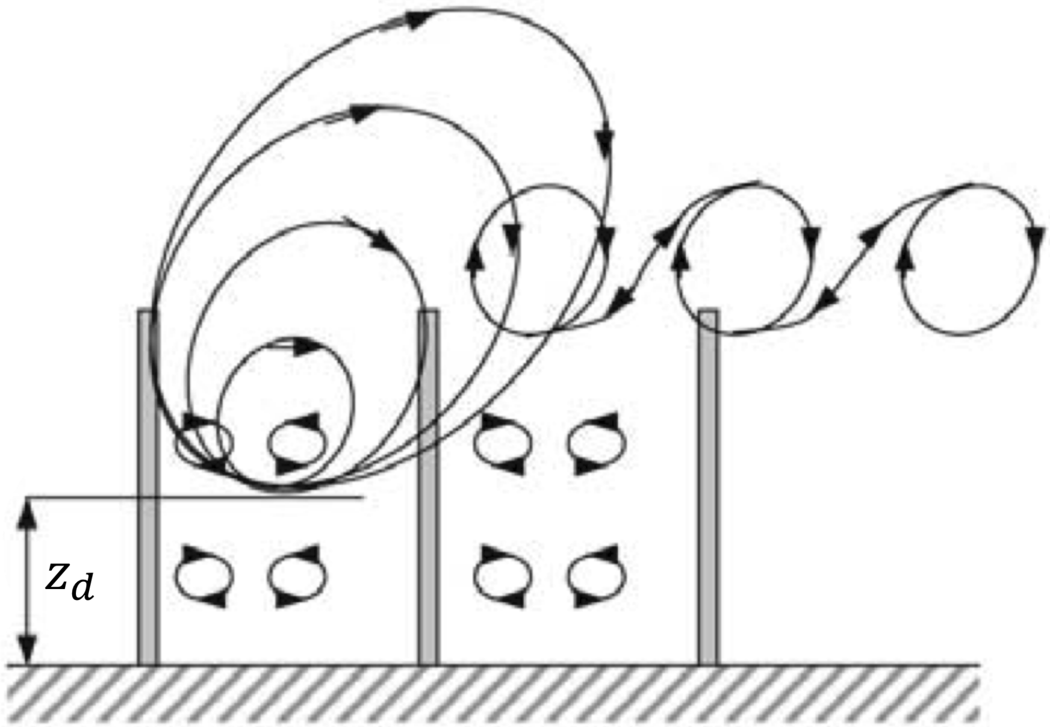


Figure 1.9: In the phenomenological model of Poggi et al. (2004), the size of vortices distribute into three categories. Far above local effects, the displaced rough wall boundary layer vortices extend up into the ISL ($z \gg 2H$). Within the canopy, local canopy geometric considerations determine the nature of the vortices. The vortices in the region at and just above the canopy top are of the mixing layer type. Figure republished and modified with permission of Springer, from Poggi et al. (2004); permission conveyed through Copyright Clearance Center, Inc.

From single-point measurements above (sparse) plant canopies, Brunet et al. (1994), J. Finnigan (2000), and Raupach et al. (1996) note that $L_x \sim H$. Shaw et al. (1995) citing limitations in Taylor's hypothesis with use of the mean velocity as a proxy for the convection velocity near canopy top suggested from spatial two-point measurements that $L_x \sim (2 - 3) \cdot H$, further supported by the work of Castro et al. (2006) over urban-type roughness (a staggered cube array). Particle image velocimetry (PIV) and laser Doppler anemometry measurements over that same staggered cube array were carried out by Reynolds and Castro (2008) to identify the dominant features above, at, and within the canopy layer. They suggest a "two-scale" behavior below $z = 1.5H$ for their wind tunnel experiments that yield a nearly four-fold difference between a large longitudinal separation trend more closely linked with outer scales and a smaller longitudinal separation trend associated with canopy-produced turbulence reported at $L_x = (0.8 - 1.5) \cdot H$, depending on lateral measurement location relative to the cubes. Within the canopy (below the active turbulence of the canopy eddies), the geometric constraints of the roughness elements reportedly reduce longitudinal motions to a near constant $L_x = 0.15H$ for $z < 0.8H$, an $\approx 85\%$ reduction of $L_x$ compared to measurements at $z = 1.2H$. At every measurement location $z < 1.2H$, the ratio of longitudinal length scale $L_x$ to the vertical length scale $L_z$ always ranged between 0.5 and 2, suggestive that eddies behave more isotropically above and within the canopy.

## 1.7 The free shear layer: a change in wind state

Any flow free from solid boundaries exhibiting a mean velocity gradient is considered a free shear flow. Both jets and wakes are classically-abstracted examples, but it is the mixing layer that undergirds the initial development of either flow and in this sense is considered a basic building block of any free shear flow (Heinrich E. Fiedler, 1998).

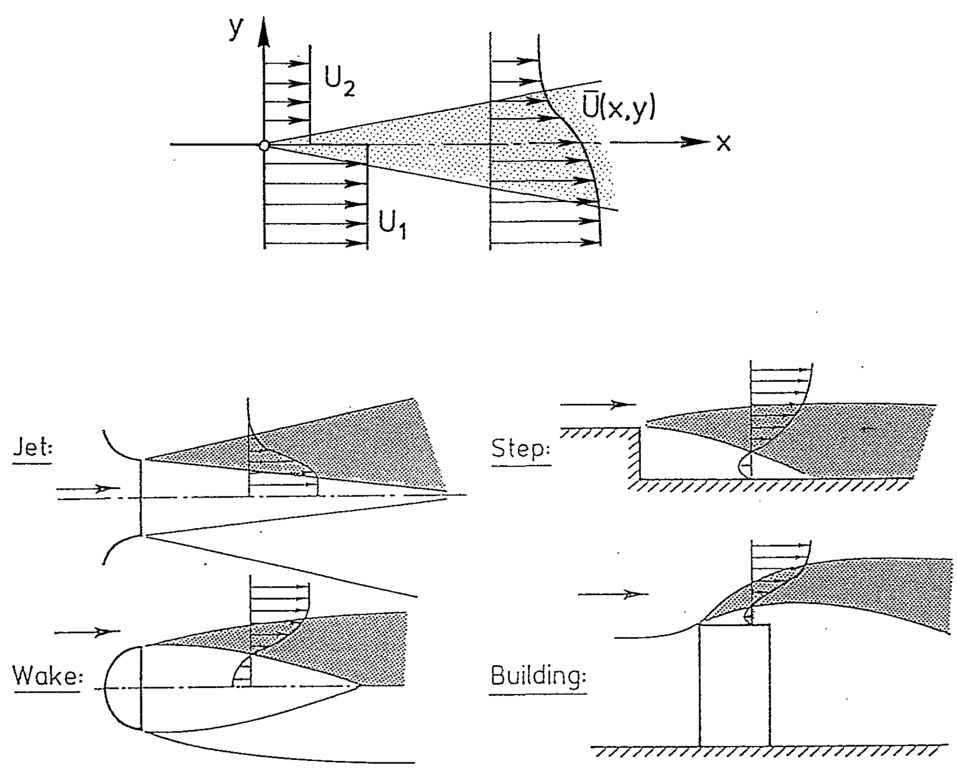


Figure 1.10: The hatched areas highlight the growth of the shear layer in the jet, wake, step, and simple building configurations. Figure republished with permission of Springer, from Heinrich E. Fiedler (1998); permission conveyed through Copyright Clearance Center, Inc.

When viewed two-dimensionally, each of the examples of fig. 1.10 conceptually initialize the wind conditions as a step input with corresponding output being that of a growing free shear layer. When the dynamics of the flyer are decoupled from the dynamics of the shear layer, passage through the shear layer can be treated as a quasi-steady gradation serving as a finite thickness division (that grows downstream) between two wind states. Then, from the point-of-view of the flyer, a discrete gust, of some obliqueness determined by the entry/exit angle of the flyer, is experienced.

**What is meant by 'discrete gust'?**

A discrete gust refers to a noticeable change in wind state encountered briefly by a flyer. It is discrete insomuchas the wind event is individually separate and distinct from an otherwise baseline flowfield and is brief in that the wind event is transitory.

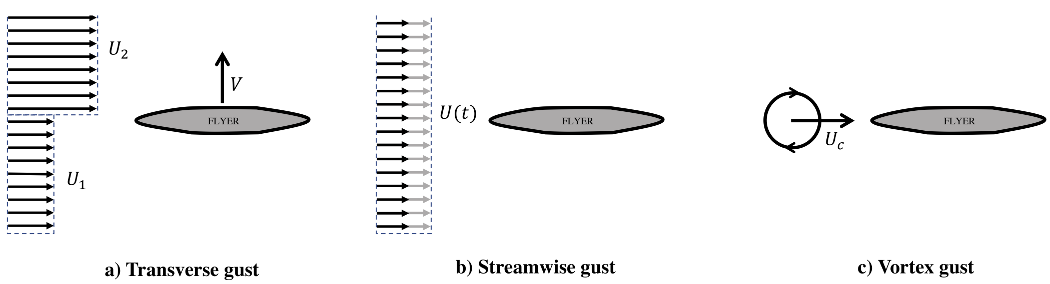


Figure 1.11: Gust types within the selected view.

Three such discrete gust abstractions are typically considered, diagrammed in fig. 1.11. *Transverse* gusts, such as updrafts in forward flight or cross-flows when ascending/descending, are characterized by their angle of incidence (i.e. direction of shearing wind relative to the flyer is taken as normal to the direction of flight) and relative magnitude of wind speed. *Streamwise* gusts that represent the instantaneous nature of changing winds near the surface, manifest as time variations in the streamwise flow, relative to the flyer; when steep, the flyer experiences a gust front. A transience (or residence time) is implied with discrete gusts, and a flyer can be thought to fly into or out of the gust encounter. Either direction can represent a significant change of state of wind speed, depending on the steepness of the gradient. Oblique flight through strong shear layers, in the two-dimensional view, represents a combination of the transverse and streamwise gust encounters. *Vortex* gust encounters are transient events that occur between gust shear layers that bound a wake, for instance, where coherent structures are shed from the surface roughness elements and are perceived by the flyer discretely.

### The domains entered

Certain classical abstractions of fig. 1.10 translate to reality better than others. For instance, it is not difficult to see the similarities between the selected view of the mountain cliffside microclimate and the geometrically idealized step configuration; based on our general understanding of step flows we may even be able to intuit the nature of the recirculation zone that would likely form in the sheltered cliffside. Further, we may convince ourselves that the shear layer developed above the tallest building in a cityscape may resemble in some way the simple building configuration, but the ideal view quickly fades when descending further into the canopy layer (CL). Within, the flowfield consists predominantly of wakes, not unlike the wake configuration of fig. 1.10, but initiated and superimposed from the many individual bluff roughness elements. Interaction with such turbulence would depend largely on the morphology of the roughness and the specific point in space considered. Though the flowfield domains into which the flyer enters and exits will vary from microclimate-to-microclimate, day-to-night, based on the roughness and with height, careful consideration elucidates a set of locally energetic and prevalent flow features (in the presence of a reasonably strong wind) warranting a closer look as candidates for experimental simulation. From this point forward, to promote a more focused conversation, canopied flows over roughness elements whose average height far exceeds the applicability of traditional boundary layer scaling techniques will be considered. To enter or leave the domains demarcated by the canopy layer boundary requires passage through the canopy-scale eddies that are active in the presence of a prevailing wind. Once within the canopy, lateral shear at the interface between superposed interacting wake and non-wake regions behind the bluff bodies accounts for lesser energetic and less coherent shear-induced finer-scale turbulence. Above the canopy layer, where the freestream velocity begins to recover, the presence of the shear layer is still felt, but not discretely as when passing through.

### Canopy shear layers - mixing layers and wakes

It is precisely the change in velocity profile coupled with the discreteness and distribution of the roughness elements that, when adopting a more local view, prompted researchers to explore the physical consequences of the observed mean velocity inflection point above vegetation canopies (e.g. Raupach et al. (1996) and J. Finnigan (2000) through field observation and J. J. Finnigan et al. (2009) through simulation) and subsequently extended to bluffer configurations in a wind tunnel (e.g., see Böhm et al., 2013; Reynolds and Castro, 2008).

If the roughness elements are tall enough and distributed so as to support a canopy flow regime, then the flow retains few of the mechanisms of wall turbulence and is better described as a flowfield over distributed obstacles. Notions of universality based on height above the surface have no bearing in this local view, as the presence of coherent structures near the canopy top supplants as a dominant flow mechanism. The surface density ultimately determines the thickness of the roughness sublayer (RSL), the region of transition between eddies linked to a height-independent length scale and eddies in the ISL that grow with distance from the displacement plane $z_d$ (i.e. height-dependent).

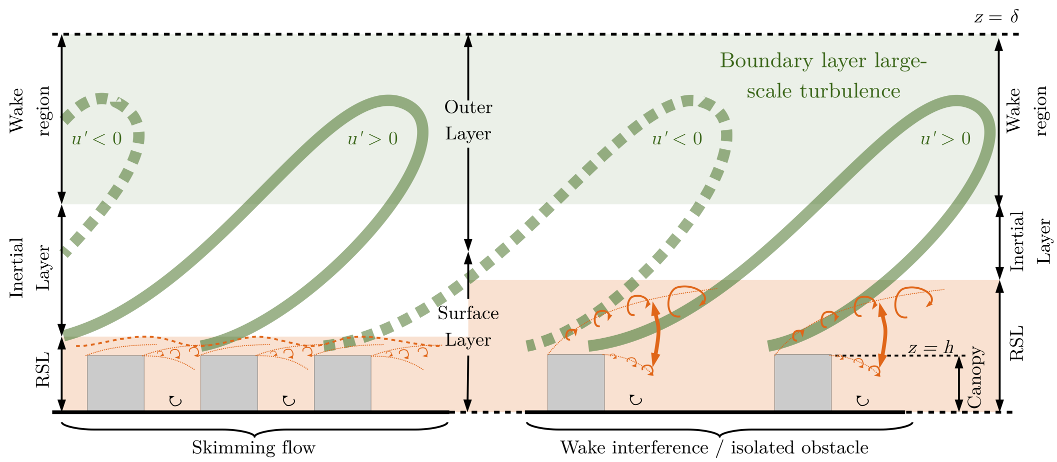


Figure 1.12: The surface roughness density determines two types of flow behaviors in the idealized uniform-height roughness configurations typically tested in wind tunnel studies. Denser configurations result in a sheltered skimming flow that decrease the effect of roughness in upper layers whereas sparser configurations increase the reach of roughness proportional to the frontal surface of the roughness elements. Meandering ‘superstructures’, representing the most energetic structures in the energy spectrum of the surface layer, reach up into the logarithmic region and scale with the boundary layer thickness $\delta$, an outer variable length scale (e.g., see Hutchins and Marusic, 2007). Figure republished with permission of Springer Nature BV, from Perret et al. (2019); permission conveyed through Copyright Clearance Center, Inc.

A simplified view of the canopy flow regime centered on the premise that the flow dynamics in the three regions immediately above, at, and within the canopy are most influenced by the presence of free shear layers with characteristic eddy length scales that are height-independent signals a major departure from traditional boundary-layer scaling techniques that focus on the energetic motions of the inertial sublayer (ISL) known to scale with height.

The instability associated with the inflection point of the mean velocity profile near canopy top, at least for winds flowing across a relatively uniform-height urban canyon (as opposed to down its streets), was observed by Christen (2005) to produce turbulence that fit well within the plane mixing layer analogy of Raupach et al. (1996) developed for vegetation canopies to explain observed differences in canopy turbulence compared to turbulence in the ISL. However illustrative, the simplified view across a dense canopy of uniform height (or of flow above or around a single obstacle in isolation) is far removed from the spatial reality of a clustered set of bluff obstacles more commonly found in the canopies of interest.

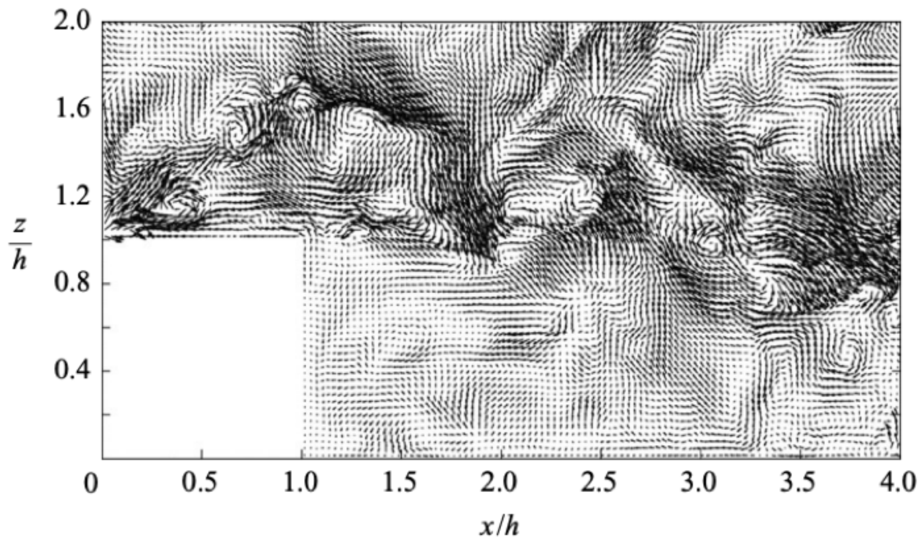


Figure 1.13: The fluctuating wind vectors over a regular array of cubic obstacles from the numeric study of Coceal et al. (2007).

A conceptual leap can be made up to a staggered or aligned array of bluff bodies as is often used in wind tunnel and numerical studies. Relatively scant data exists for within-canopy three-dimensional flows, however, Davidson et al. (1996) for a cube-obstacle array in a wind tunnel calculated turbulence statistics to compare staggered and aligned configurations and found that within the array canopy, the turbulence would be smaller scale with higher turbulence intensity, citing the reduction of Langrangian time scales as evidence. Studies done by Böhm et al. (2013) with automotive light globes in a wind tunnel setting called into question the general dynamic significance of the mixing layer analogy applied to an urban-like environment of staggered bluff obstacles. A key difference observed was a more pronounced contribution to the energy spectrum at scales much smaller than the coherent structures initiated at the inflection point, accounted for by the wake-introduced turbulence kinetic energy. As such, it can be expected that turbulence within the canopy layer (CL) locally has the characteristics of superimposed quasi-coherent wakes initiated from the individual roughness elements, observed to be about 1/5 the scale of the mixing layer type eddies at the canopy inflection point. This significant scale separation motivates treatment of the canopy as three distinctive flow regimes characterized by superimposed wakes within the canopy, mixing layer type coherent structures at the canopy top and a region above where the dynamics transition from a dependence on the smaller eddies at the canopy top to the larger height-dependent eddies of the ISL. It would appear, then, that to simulate idealized versions of flowfields across the canopied surfaces, the mixing layer will play a prominent role, whether initiated along a plane or shaped into the development of superposed wakes.

## 1.8 The regions of interest and approach methodology

For the regions of interest within the surface layer, mean vertical velocities are assumed much smaller than horizontal ones so that treatment of the problem is sufficiently one-dimensional when aligned with the prevailing wind. By rotating the view around the z-axis to always be oriented in the compass-based direction of mean motions, the velocity field is represented as:

$$\begin{aligned} u &= \overline{u}_h + u'_h \\ v &= v' \\ w &= w' \end{aligned} \tag{1.12}$$

with $\overline{u}_h$ typically taken as the mean horizontal wind speed as measured by a probe in fixed coordinates as $\overline{u}_h = \sqrt{\overline{u}^2 + \overline{v}^2}$, with $\overline{w}^2 \approx 0$. This assumption certainly holds in the ISL and approximately holds in the RSL when far enough from local effects, particularly when roughness elements at the surface are rather short and uniformly distributed. From this point forward, the subscript "h" indicating a horizontal wind will be dropped and $u, v, w$ will be understood to be the longitudinal, lateral, and vertical velocity components, respectively. The gap in the spectral distributions of wind, like that shown in fig. 1.7, enables the fluctuating portion of the wind spectra to be isolated from the mean motions. By taking suitably long averages (say, thirty minutes to an hour) of all terms in eq. (1.3) and then subtracting these averages from eq. (1.3) yields the Navier-Stokes equations for the gust portions of the wind spectra, which would be parameterized by mean velocity (and mean temperature) profiles with altitude. Far above the effects of roughness in the ISL, eq. (1.9) would be one such candidate altitude-profile for mean winds and within a uniform-height, long stretching canopy, perhaps eq. (1.10) could be used with not too great a loss in accuracy. Whatever form of these mean velocity profile equations is ultimately selected, an inflection point near canopy top ensures that any similarity theory dependent solely on dynamic-scaling with height will miss the important dominant flow mechanism of the coherent structures generated within the local microclimate control volume views adopted herein.

For certain terrain-following flows when the atmosphere is particularly stable (common at night), turbulence, though continuous, is weak and waves are ubiquitous. Thus, a more encompassing decomposition for the longitudinal velocity component in this case would be $u = \overline{u} + u' + \tilde{u}$, which further parses the wave contributions $\tilde{u}$ from the turbulent fluctuations $u'$ in the microscale portion of the energy spectrum. A short-hand that preserves the potential for decomposing the fluctuating component between a random and deterministic periodic component as the situation calls for is given as

$$u = \overline{u} + u^{\nsim} \tag{1.13}$$

where $u^{\nsim} = u' + \tilde{u}$. In general, these atmospheric wave motions push energy to the mesoscale portion of the spectrum far from the spectral overlaps of interest, but eq. (2.15) is included here nonetheless because certain techniques for turbulence generation in multi-source wind tunnels leverage discrete oscillatory forcings to bump energy into specific frequency bands, and is therefore applicable in those analyses contexts.

Because traditional wind tunnel testing of fix-mounted flyers in a steady airstream with low turbulence intensity or the quasi-static dynamic modeling approach in control design is unlikely to properly account for the transient and more localized effects of gusts in the RSL, an iterative free-flight experimental approach where the flyer (e.g. machine) *learns* from exposure to the simulated environment is proposed. With a focus on flight performance during the presence of reasonably strong winds near the surface (i.e. gustiness that approaches the flight speed capabilities of the near-surface flyers), techniques for the simulation of the spectrum of horizontal winds in a laboratory setting are explored as a principal step toward that aim. A frequency-domain representation will often be employed as that will inevitably permit a direct comparison of the spectral features of a flyer of interest with the spectral content of the environmental disturbances. It is important to note that the goal of this dissertation is not a true-to-form simulation of the spectral behavior of disturbances in the atmospheric surface layer, but rather on simulation of the most energetic disturbances within a specific spectral range likely to overlap frequency regimes important to the design, testing, and understanding of flyer-specific features, such as flight-control, actuation, and structural integrity.

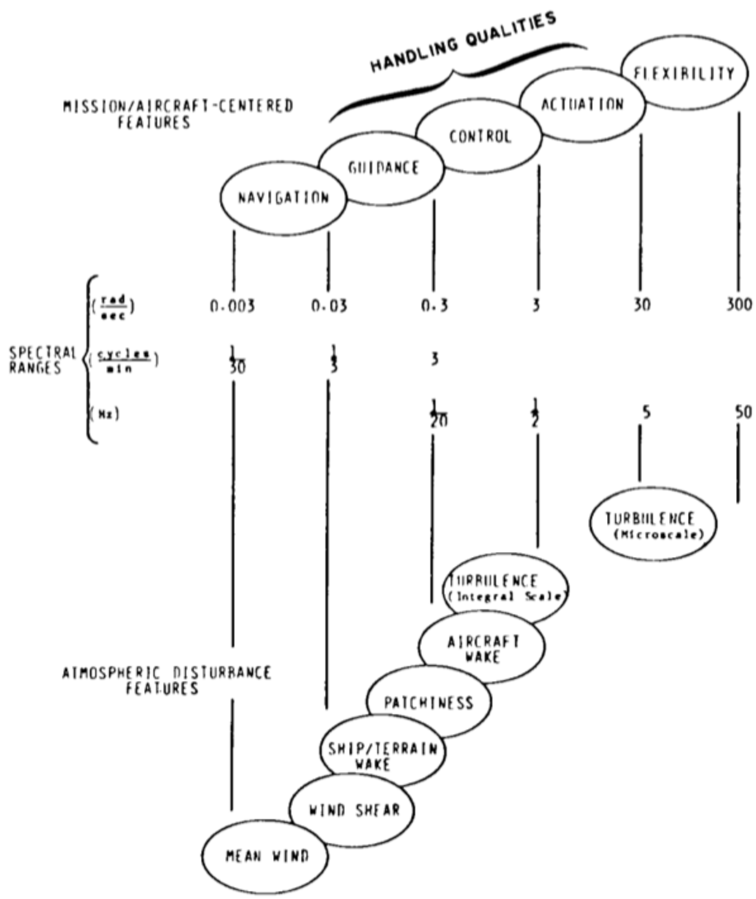


Figure 1.14: Approximate frequency regimes of overlap for flyer-specific and atmospheric disturbance features, from MIL-STD-1797A.

## 1.9 Objectives: the winds ahead

Though extensive variability exists within the microclimates explored, some narrowing of the view enables the development of a framework for the simulation of atmospheric-like disturbances near the surface in the confines of a laboratory setting with the goal of exposing, studying, and testing flyers of interest within physical models of the environment. By identifying the characteristic features of a given local environment most likely to impact the dynamics of a flyer of interest, an analogous flow configuration is set out to be created that *resembles* flight through the atmosphere near the surface at relevant time and length scales. Repeated exposure to suitable forcing functions enables flyers to learn to navigate and negotiate challenging environments well-before encountering them in the real-world.

The perception of the disturbance environment by the flyer depends largely on its location in space near the surface relative to the built-up environment, when present. Far from local effects, atmospheric turbulence in the spectral overlap of interest is essentially isotropic and well-described by the theoretical model of Kármán (see eq. (1.11)). However, for control volumes zoomed in and centered at the canopy top, three identifiable flow regimes based on the relative effects and implications of an observed inflection point of the mean velocity profile were discussed. It was argued that free shear layers are prevalent in the disturbance flowfields that merit simulation in the physical laboratory environment, both for exploration of the mixing-layer type flowfields at or near the observed canopy inflection points, but also as a fundamental building block for evolved superimposed wake flowfields within the canopy.

Generation of mixing layers is given extensive treatment in Chapter III, through use of a modular, multi-source wind tunnel introduced in Chapter II and further described in appendix A. Characteristics of basic flow modalities are presented along with perturbation techniques driven solely by software toward the generation of continuous-turbulence velocity fields in Chapter IV. A framework of comparison for these high-Re flows is explored thereafter in Chapter V. A brief exploration of the effect of various perturbation techniques on core flowfields is given in appendix D. The objectives of the study are listed below:

1. Establish the conceptual framework and principal characteristics of a multi-source wind tunnel to determine its suitability for the generation of environmental disturbances (i.e. random and discrete gusts) likely to be encountered near the surface

2. Characterize the splitterplate-less dual- and triple-stream mixing layers enabled by the discrete partitioning and individual addressability of the fan units within the multi-source wind tunnel environment

3. Showcase continuous turbulence generation techniques built on the premise of shearing velocity distributions at the fan array exit plane

4. Develop a framework of comparison for the simulated flowfields of interest